Supplemental Information

Analysis of the distributions of hourly NO_2 concentrations contributing to annual average NO_2 concentrations across the European monitoring network between 2000 and 2014

C.S. Malley, E. von Schneidemesser, S. Moller, C.F. Braban, W.K. Hicks, M.R. Heal

This Supplemental Information contains 19 figures:

Figure S1: The proportion of within-cluster variance explained as a function of number of clusters for monitoring sites with 2010-2014 average annual NO_2 concentrations between 60 and 70 μg m^{-3}. The red dot indicates the number of clusters into which sites were grouped.

Figure S2: The proportion of within-cluster variance explained as a function of number of clusters for monitoring sites with 2010-2014 average annual NO_2 concentrations between 50 and 60 μg m^{-3}. The red dot indicates the number of clusters into which sites were grouped.

Figure S3: The proportion of within-cluster variance explained as a function of number of clusters for monitoring sites with 2010-2014 average annual NO_2 concentrations between 40 and 50 μg m^{-3}. The red dot indicates the number of clusters into which sites were grouped.

Figure S4: The proportion of within-cluster variance explained as a function of number of clusters for monitoring sites with 2010-2014 annual NO_2 concentrations between 30 and 40 μg m^{-3}. The red dot indicates the number of clusters into which sites were grouped.

Figure S5: The proportion of within-cluster variance explained as a function of number of clusters for monitoring sites with 2010-2014 annual NO_2 concentrations between 20 and 30 μg m^{-3}. The red dot indicates the number of clusters into which sites were grouped.

Figure S6: The proportion of within-cluster variance explained as a function of number of clusters for monitoring sites with 2010-2014 annual NO_2 concentrations between 10 and 20 μg m^{-3}. The red dot indicates the number of clusters into which sites were grouped.

Figure S7: The proportion of within-cluster variance explained as a function of number of clusters for monitoring sites with 2010-2014 annual NO_2 concentrations between 0 and 10 μg m^{-3}. The red dot indicates the number of clusters into which sites were grouped.

Figure S8: Map of countries assigned to the European regions used in Figure 3.

Figure S9: Map of sites with 2010-2014 annual NO_2 concentrations (NO_{2AA}) between 60-70 μg m^{-3}, grouped into clusters demarcating distinct variations in monthly, hour of day, and hourly NO_2 concentration bin contributions to 2010-2014 NO_{2AA}.

Figure S10: Map of sites with 2010-2014 annual NO_2 concentrations (NO_{2AA}) between 50-60 μg m^{-3}, grouped into clusters demarcating distinct variations in monthly, hour of day, and hourly NO_2 concentration bin contributions to 2010-2014 NO_{2AA}.

Figure S11: Map of sites with 2010-2014 annual NO_2 concentrations (NO_{2AA}) between 40-50 μg m^{-3}, grouped into clusters demarcating distinct variations in monthly, hour of day, and hourly NO_2 concentration bin contributions to 2010-2014 NO_{2AA}.

Figure S12: Map of sites with 2010-2014 annual NO_2 concentrations (NO_{2AA}) between 30-40 μg m^{-3}, grouped into clusters demarcating distinct variations in monthly, hour of day, and hourly NO_2 concentration bin contributions to 2010-2014 NO_{2AA}.

Figure S13: Map of sites with 2010-2014 annual NO_2 concentrations (NO_{2AA}) between 20-30 μg m^{-3}, grouped into clusters demarcating distinct variations in monthly, hour of day, and hourly NO_2 concentration bin contributions to 2010-2014 NO_{2AA}.

Figure S14: Map of sites with 2010-2014 annual NO_2 concentrations (NO_{2AA}) between 10-20 μg m^{-3}, grouped into clusters demarcating distinct variations in monthly, hour of day, and hourly NO_2 concentration bin contributions to 2010-2014 NO_{2AA}.

Figure S15: Map of sites with 2010-2014 annual NO_2 concentrations (NO_{2AA}) between 0-10 μg m^{-3}, grouped into clusters demarcating distinct variations in monthly, hour of day, and hourly NO_2 concentration bin contributions to 2010-2014 NO_{2AA}.

Figure S16: Comparison of the direction and magnitude of the trend in annual NO_2 concentrations between 2000 and 2014 at 259 sites across Europe using the Theil-Sen statistic and first order autoregressive (AR(1)) model.

Figure S17: Magnitude and significance of trend in annual average NO_2 concentrations between 2000 and 2014, with sites separated into panels based on 2010-2014 average annual NO_2 concentrations (NO_{2AA}). The fill colour in each point denotes the magnitude and direction of the Theil-Sen trend at a site, and the outer colour denotes whether the trend was statistically significant ($p \leq 0.05$, green), or not statistically significant ($p > 0.05$, orange). Trend estimates were calculated using the Theil-Sen statistic and block bootstrapping.

Figure S18: Proportion of sites with significant decreasing (blue), increasing (red) ($p \leq 0.05$), and non-significant (grey) trends in the monthly percentage contribution to annual average NO_2 between 2000 and 2014, for sites with 2010-2014 average annual NO_2 concentrations (NO_{2AA}) of a) >80 μg m^{-3}, b) 60-70 μg m^{-3}, c) 50-60 μg m^{-3}, d) 40-50 μg m^{-3}, 30-40 μg m^{-3}, 20-30 μg m^{-3}, 10-20 μg m^{-3}, 0-10 μg m^{-3}. Trend estimates were calculated using the Theil-Sen statistic and block bootstrapping. The black line represents the division between decreasing and increasing trends within the non-significant bar.

Figure S19: Proportion of sites with significant decreasing (blue), increasing (red) ($p \leq 0.05$), and non-significant (grey) trends in the percentage contribution of each hour of day to annual average NO_2 between 2000 and 2014, for sites with 2010-2014 average annual NO_2 concentrations (NO_{2AA}) of a) >80 μg m^{-3}, b) 60-70 μg m^{-3}, c) 50-60 μg m^{-3}, d) 40-50 μg m^{-3}, 30-40 μg m^{-3}, 20-30 μg m^{-3}, 10-20 μg m^{-3}, 0-10

μg m^{-3}. Trend estimates were calculated using the Theil-Sen statistic and block bootstrapping. The black line represents the division between decreasing and increasing trends within the non-significant bar.

Figure S20: Proportion of sites with significant decreasing (blue), increasing (red) ($p < 0.05$), and non-significant (grey) trends in the percentage contribution from hourly NO_2 concentrations in 5 μg m^{-3} bins to annual average NO_2 between 2000 and 2014, for sites with 2010-2014 average annual NO_2 concentrations (NO_{2AA}) of a) >80 μg m^{-3}, b) 60-70 μg m^{-3}, c) 50-60 μg m^{-3}, d) 40-50 μg m^{-3}, 30-40 μg m^{-3}, 20-30 μg m^{-3}, 10-20 μg m^{-3}, 0-10 μg m^{-3}. Trend estimates were calculated using the Theil-Sen statistic and block bootstrapping. The black line represents the division between decreasing and increasing trends within the non-significant bar.

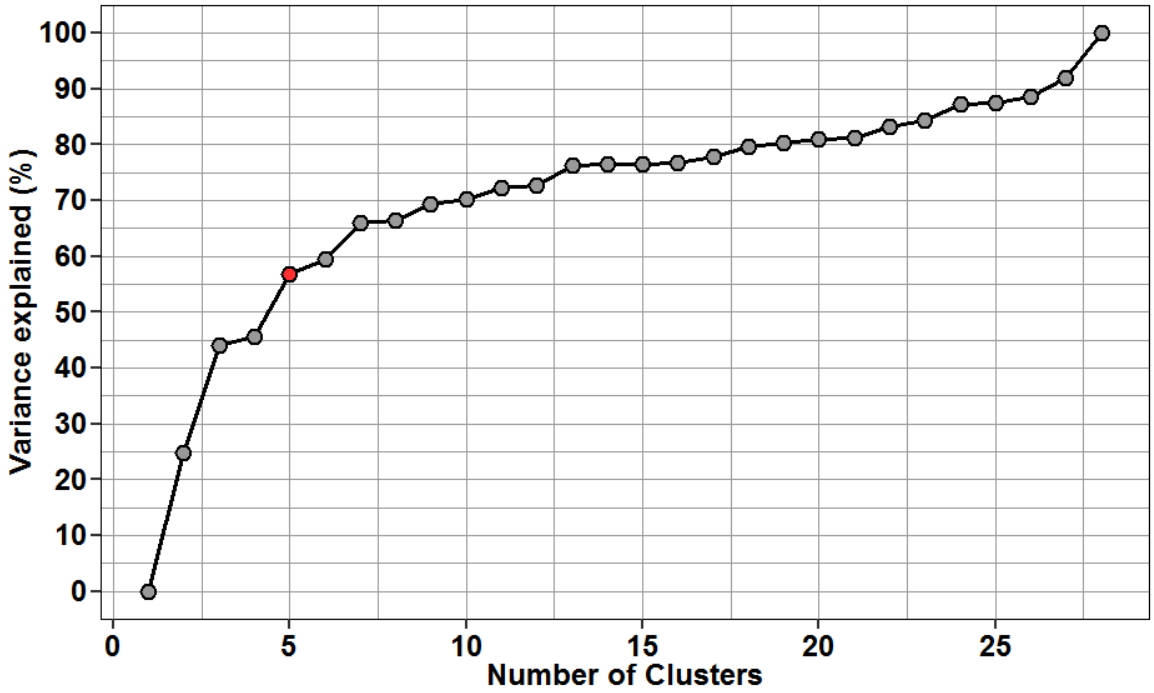

Figure S1: The proportion of within-cluster variance explained as a function of number of clusters for monitoring sites with 2010-2014 average annual NO_2 concentrations between 60 and 70 µg m^{-3}. The red dot indicates the number of clusters into which sites were grouped.

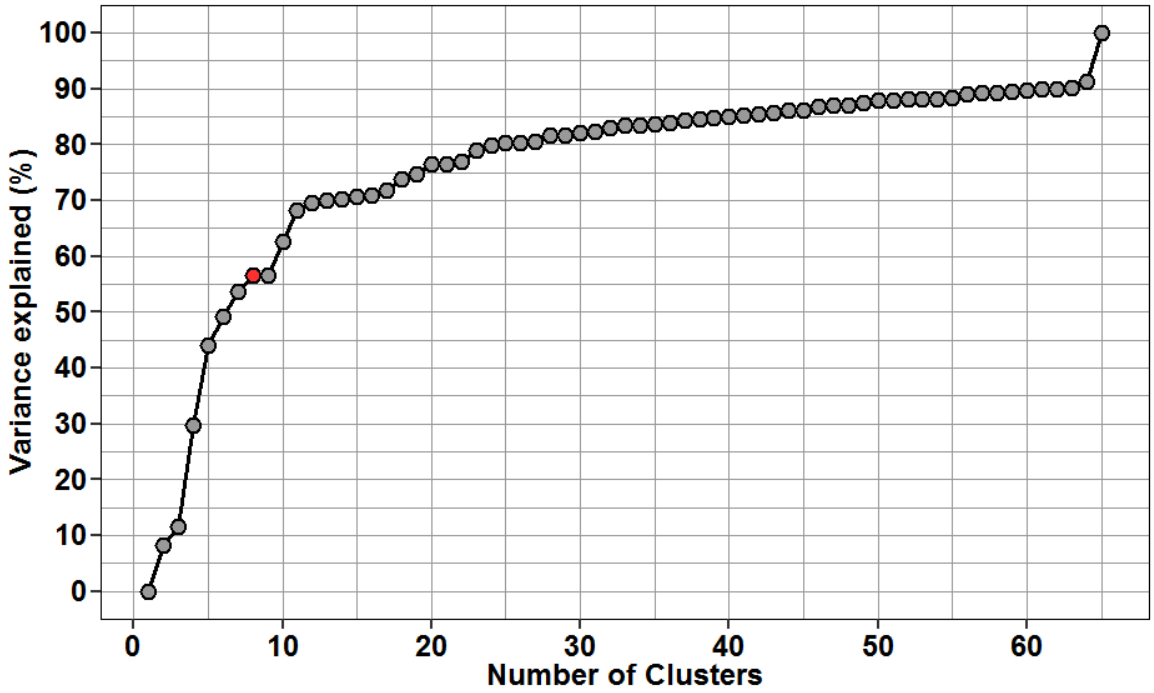

Figure S2: The proportion of within-cluster variance explained as a function of number of clusters for monitoring sites with 2010-2014 average annual NO_2 concentrations between 50 and 60 µg m^{-3}. The red dot indicates the number of clusters into which sites were grouped.

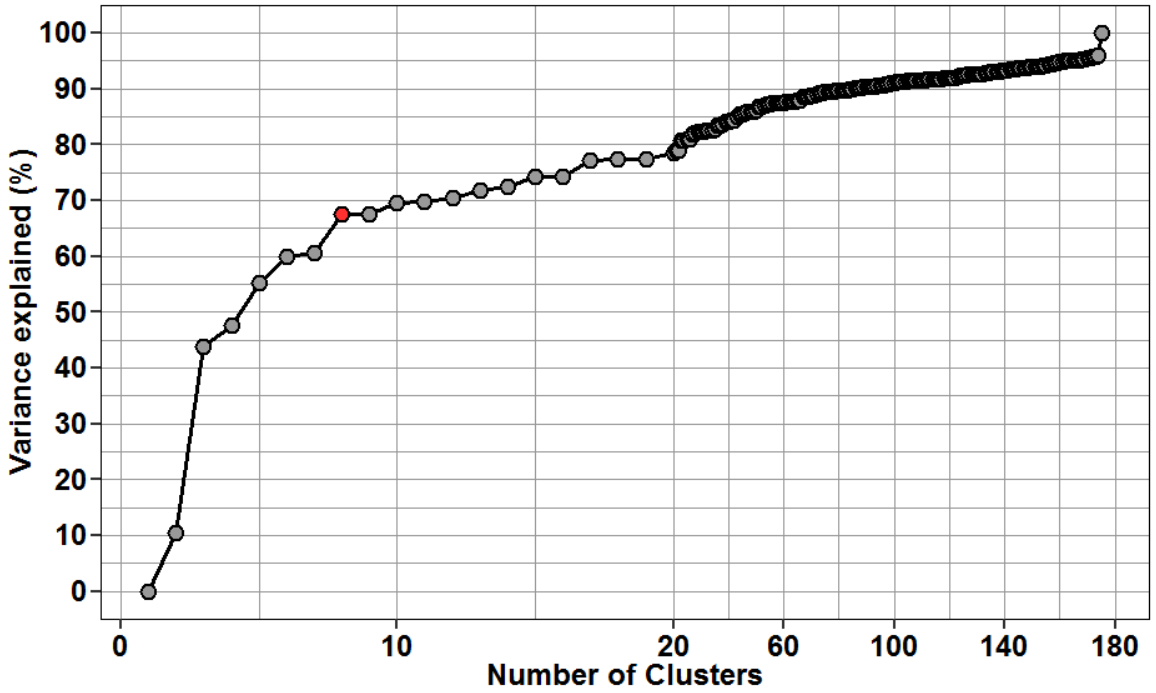

Figure S3: The proportion of within-cluster variance explained as a function of number of clusters for monitoring sites with 2010-2014 average annual NO_2 concentrations between 40 and 50 µg m^{-3}. The red dot indicates the number of clusters into which sites were grouped.

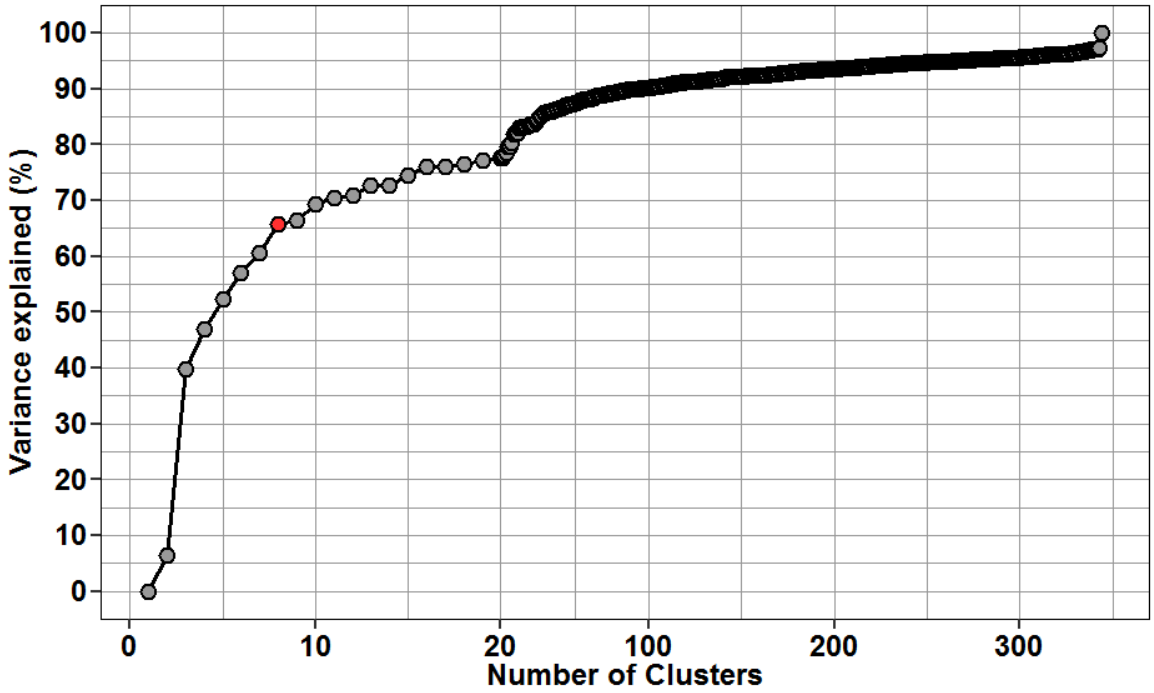

Figure S4: The proportion of within-cluster variance explained as a function of number of clusters for monitoring sites with 2010-2014 annual NO_2 concentrations between 30 and 40 µg m^{-3}. The red dot indicates the number of clusters into which sites were grouped.

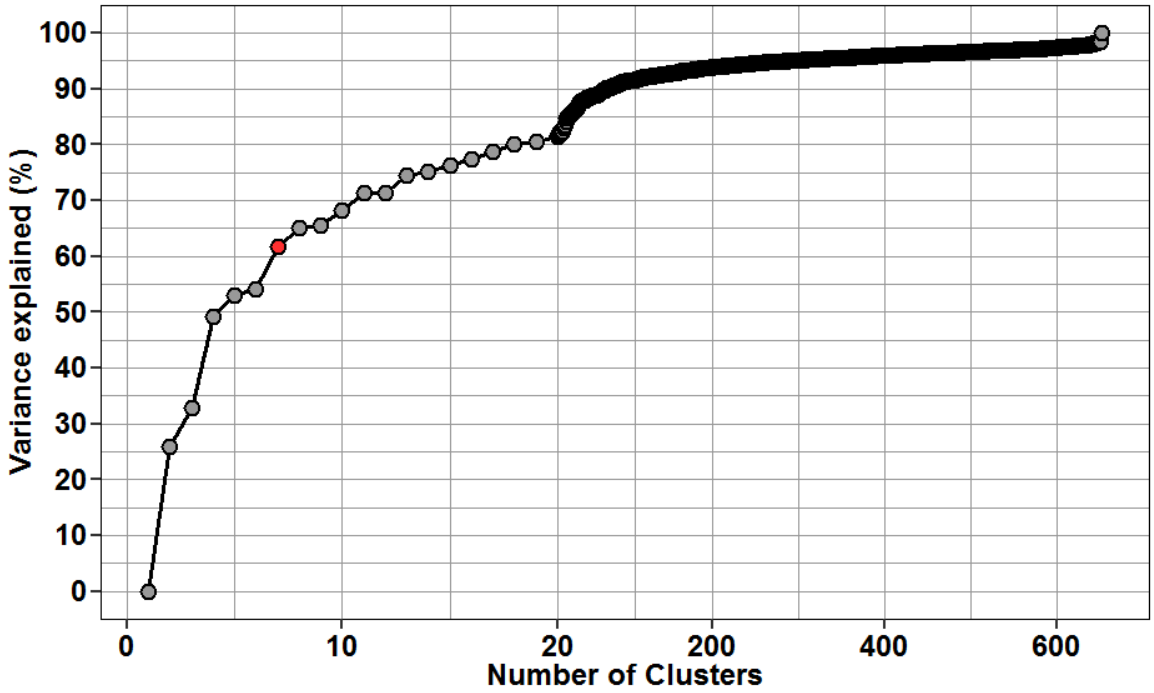

Figure S5: The proportion of within-cluster variance explained as a function of number of clusters for monitoring sites with 2010-2014 annual NO_2 concentrations between 20 and 30 µg m^{-3}. The red dot indicates the number of clusters into which sites were grouped.

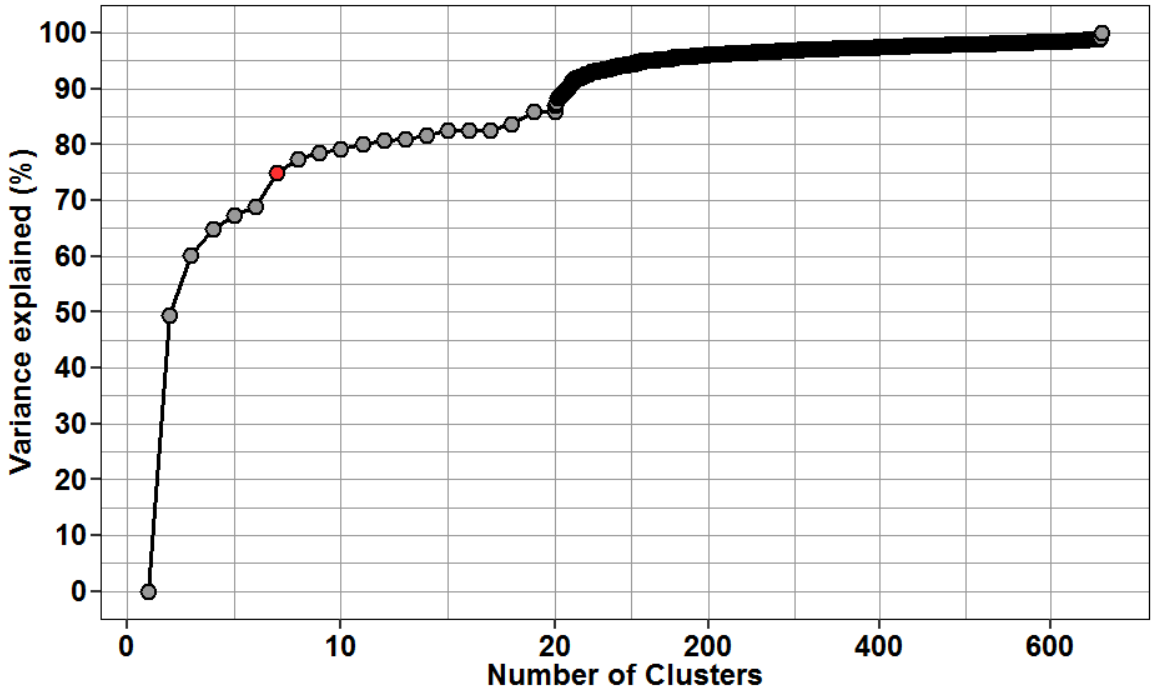

Figure S6: The proportion of within-cluster variance explained as a function of number of clusters for monitoring sites with 2010-2014 annual NO_2 concentrations between 10 and 20 μg m^{-3}. The red dot indicates the number of clusters into which sites were grouped.

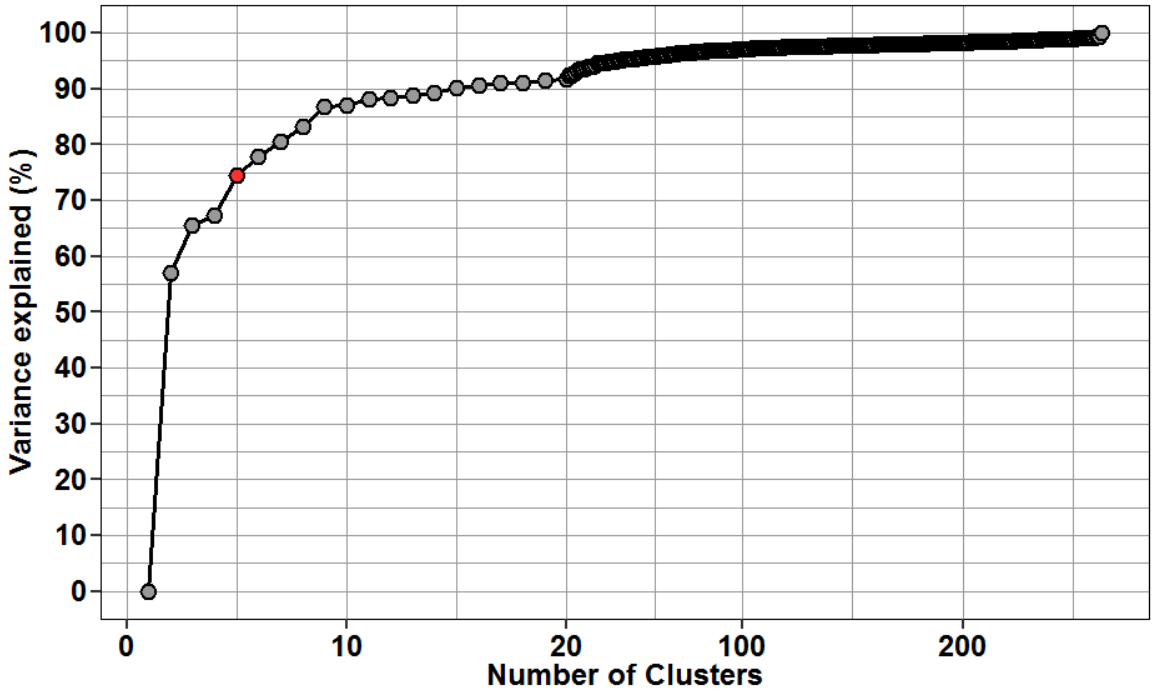

Figure S7: The proportion of within-cluster variance explained as a function of number of clusters for monitoring sites with 2010-2014 annual NO_2 concentrations between 0 and 10 µg m^{-3}. The red dot indicates the number of clusters into which sites were grouped.

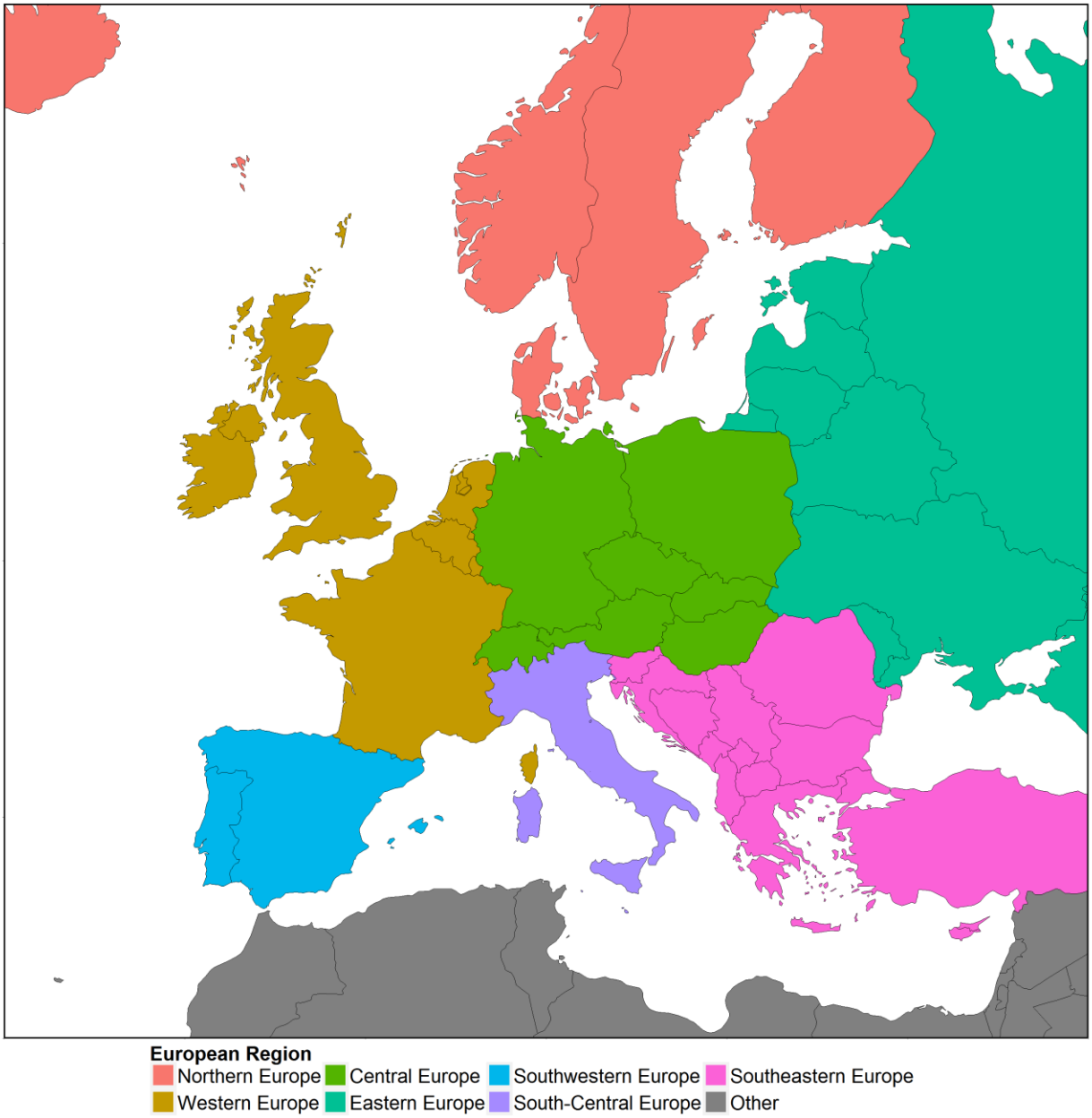

Figure S8: Map of countries assigned to the European regions used in Figure 3.

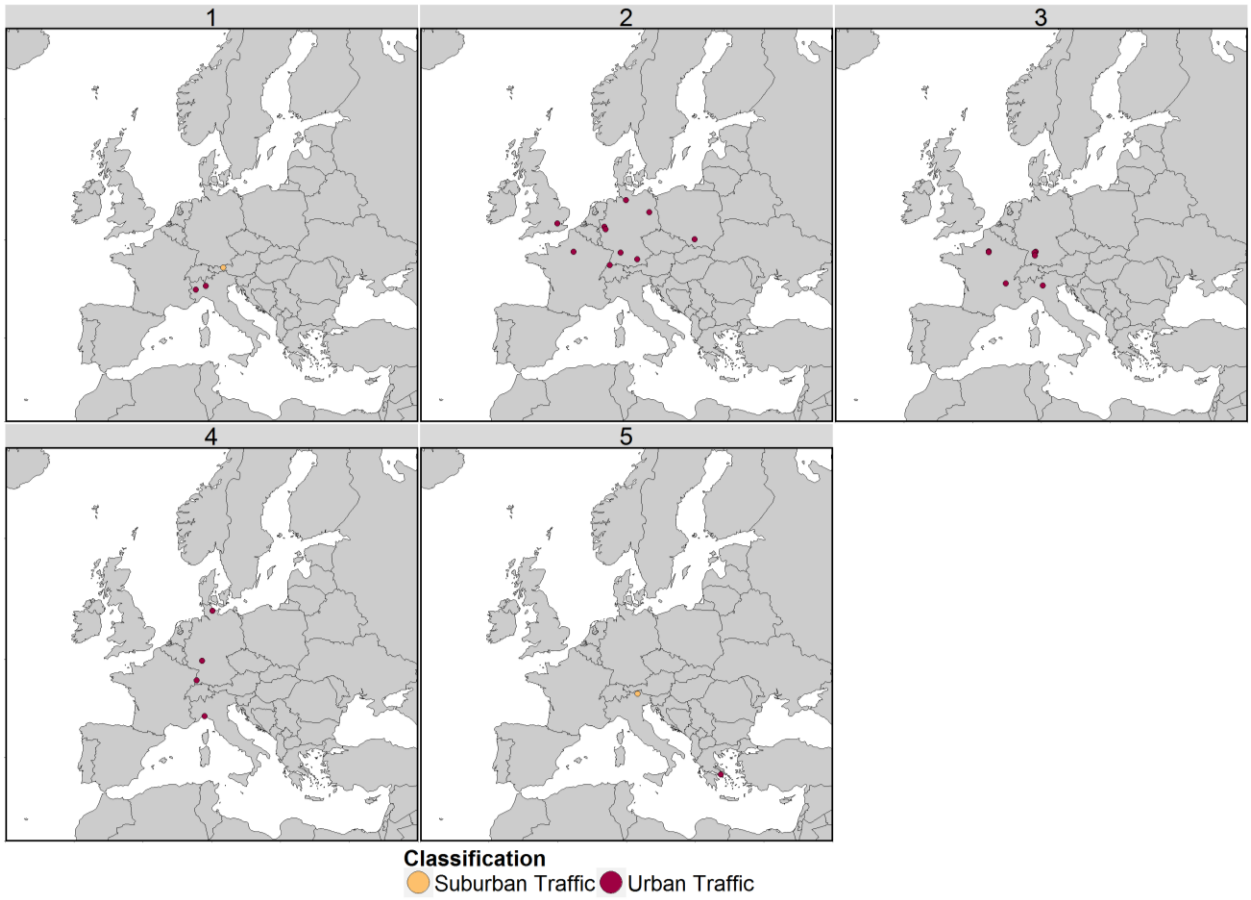

Figure S9: Map of sites with 2010-2014 annual NO_2 concentrations (NO_{2AA}) between 60-70 µg m^{-3}, grouped into clusters demarcating distinct variations in monthly, hour of day, and hourly NO_2 concentration bin contributions to 2010-2014 NO_{2AA}.

Figure S10: Map of sites with 2010-2014 annual NO_2 concentrations (NO_{2AA}) between 50-60 µg m^{-3}, grouped into clusters demarcating distinct variations in monthly, hour of day, and hourly NO_2 concentration bin contributions to 2010-2014 NO_{2AA}.

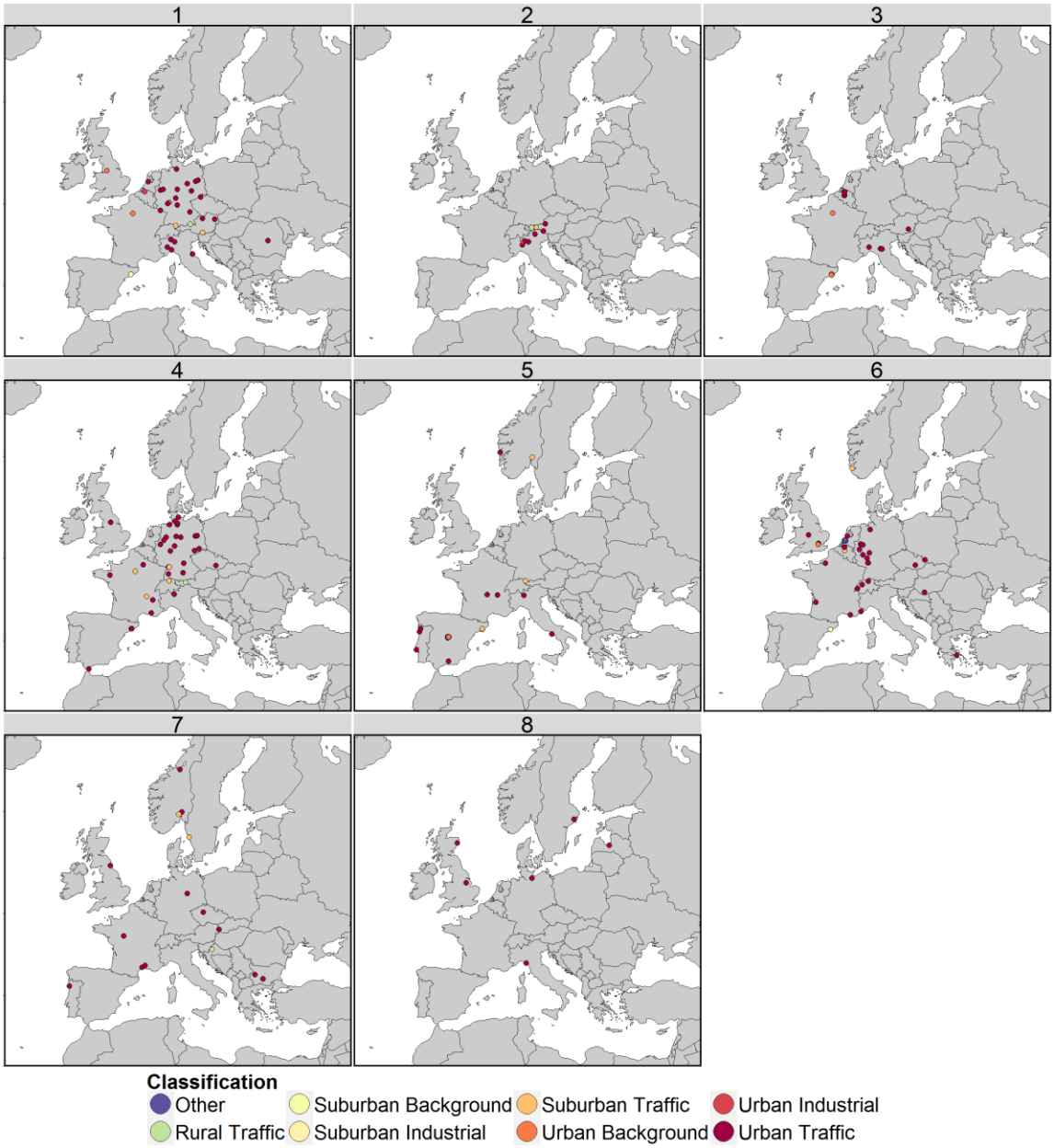

Figure S11: Map of sites with 2010-2014 annual NO_2 concentrations (NO_{2AA}) between 40-50 µg m^{-3}, grouped into clusters demarcating distinct variations in monthly, hour of day, and hourly NO_2 concentration bin contributions to 2010-2014 NO_{2AA}.

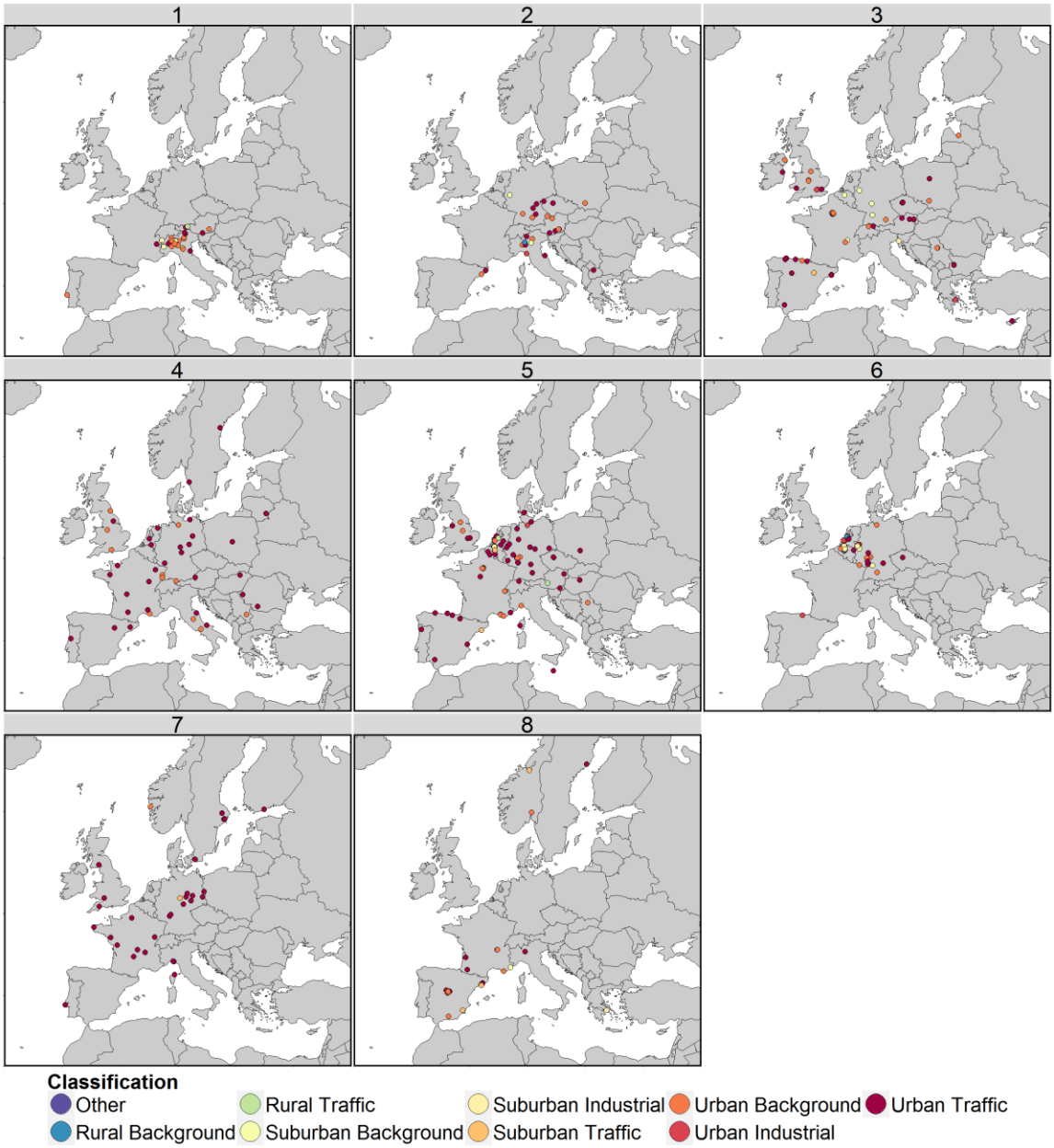

Figure S12: Map of sites with 2010-2014 annual NO_2 concentrations (NO_{2AA}) between 30-40 µg m^{-3}, grouped into clusters demarcating distinct variations in monthly, hour of day, and hourly NO_2 concentration bin contributions to 2010-2014 NO_{2AA}.

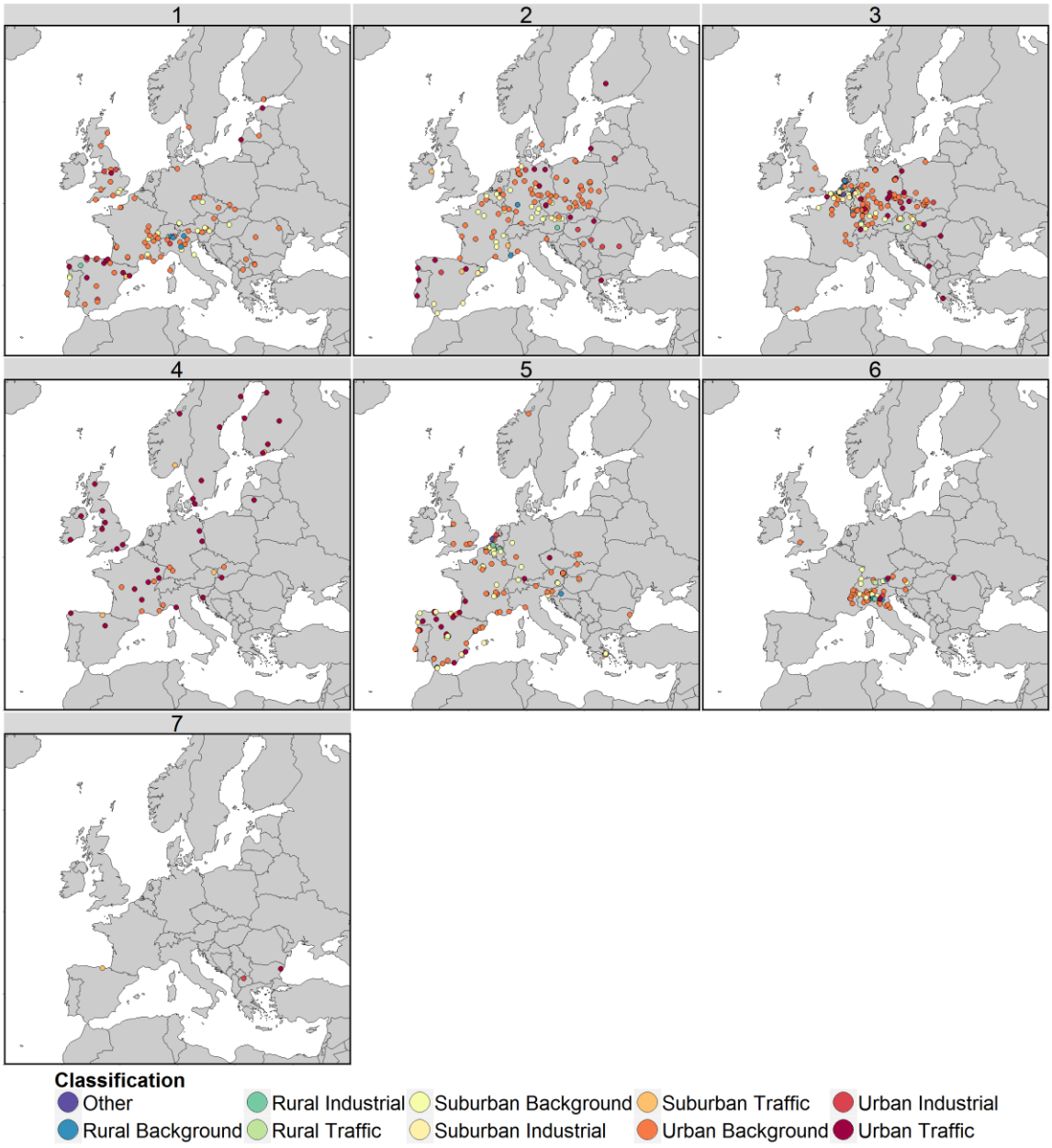

Figure S13: Map of sites with 2010-2014 annual NO_2 concentrations (NO_{2AA}) between 20-30 µg m^{-3}, grouped into clusters demarcating distinct variations in monthly, hour of day, and hourly NO_2 concentration bin contributions to 2010-2014 NO_{2AA}.

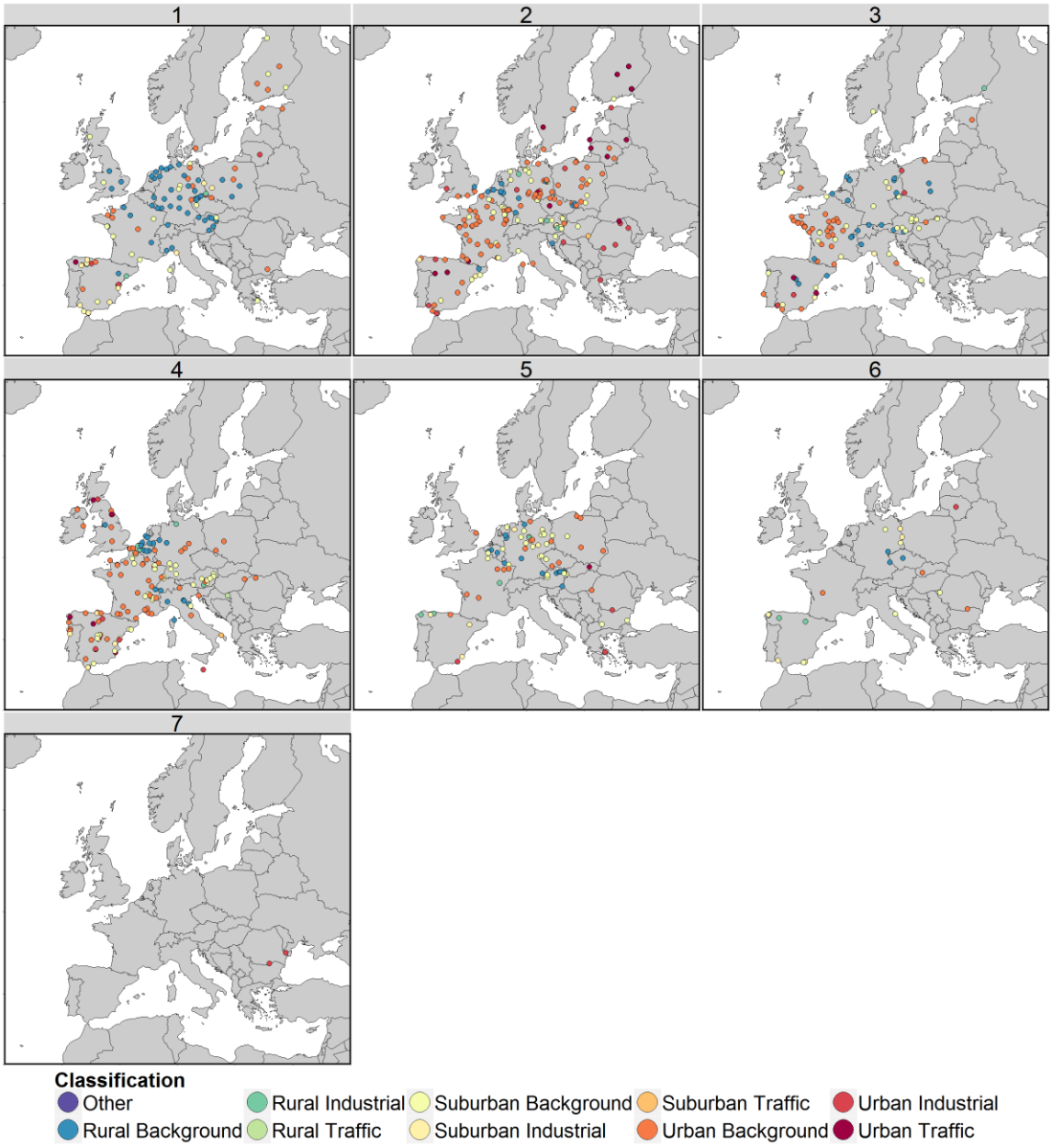

Figure S14: Map of sites with 2010-2014 annual NO_2 concentrations (NO_{2AA}) between 10-20 µg m^{-3}, grouped into clusters demarcating distinct variations in monthly, hour of day, and hourly NO_2 concentration bin contributions to 2010-2014 NO_{2AA}.

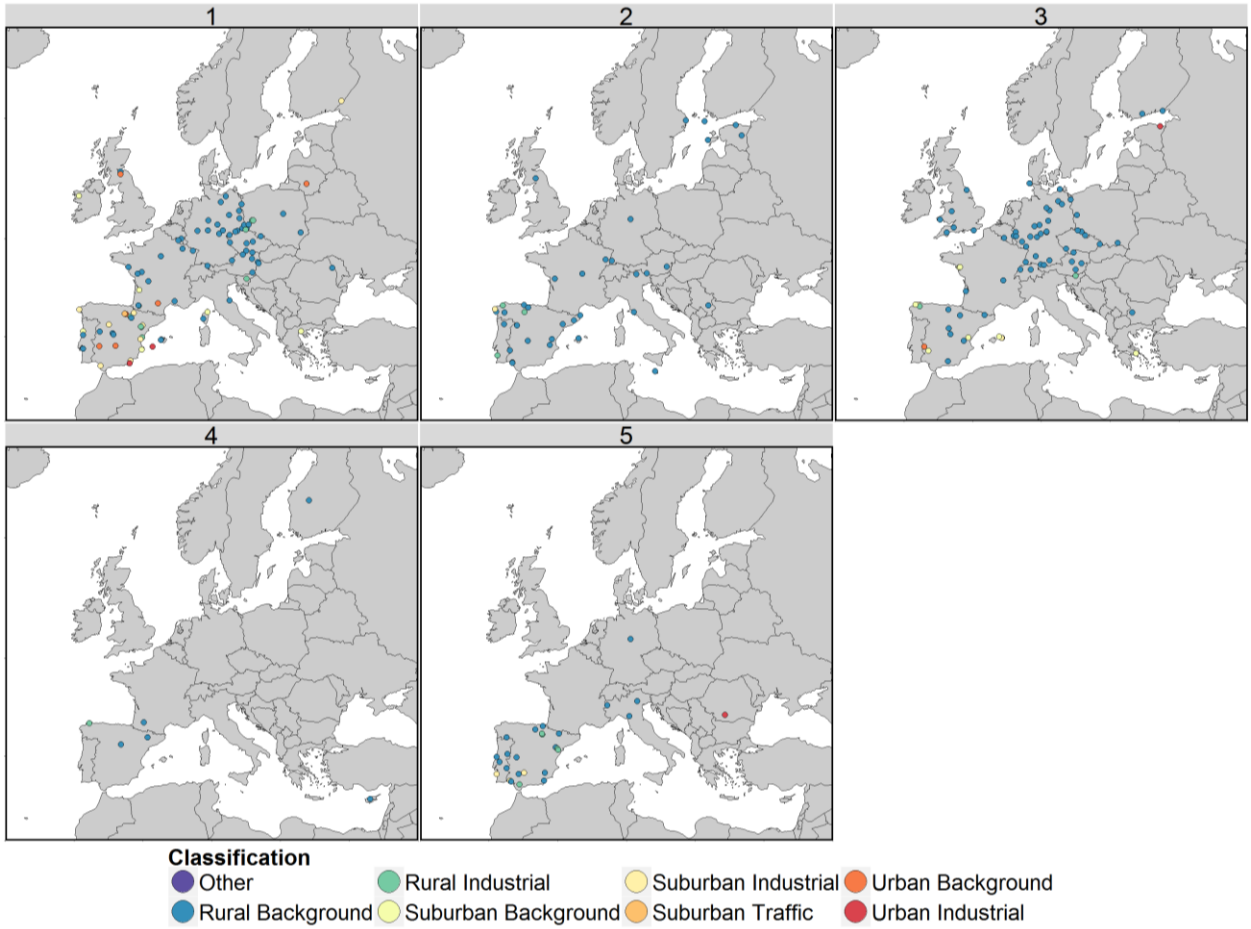

Figure S15: Map of sites with 2010-2014 annual NO_2 concentrations (NO_{2AA}) between 0-10 µg m^{-3}, grouped into clusters demarcating distinct variations in monthly, hour of day, and hourly NO_2 concentration bin contributions to 2010-2014 NO_{2AA}.

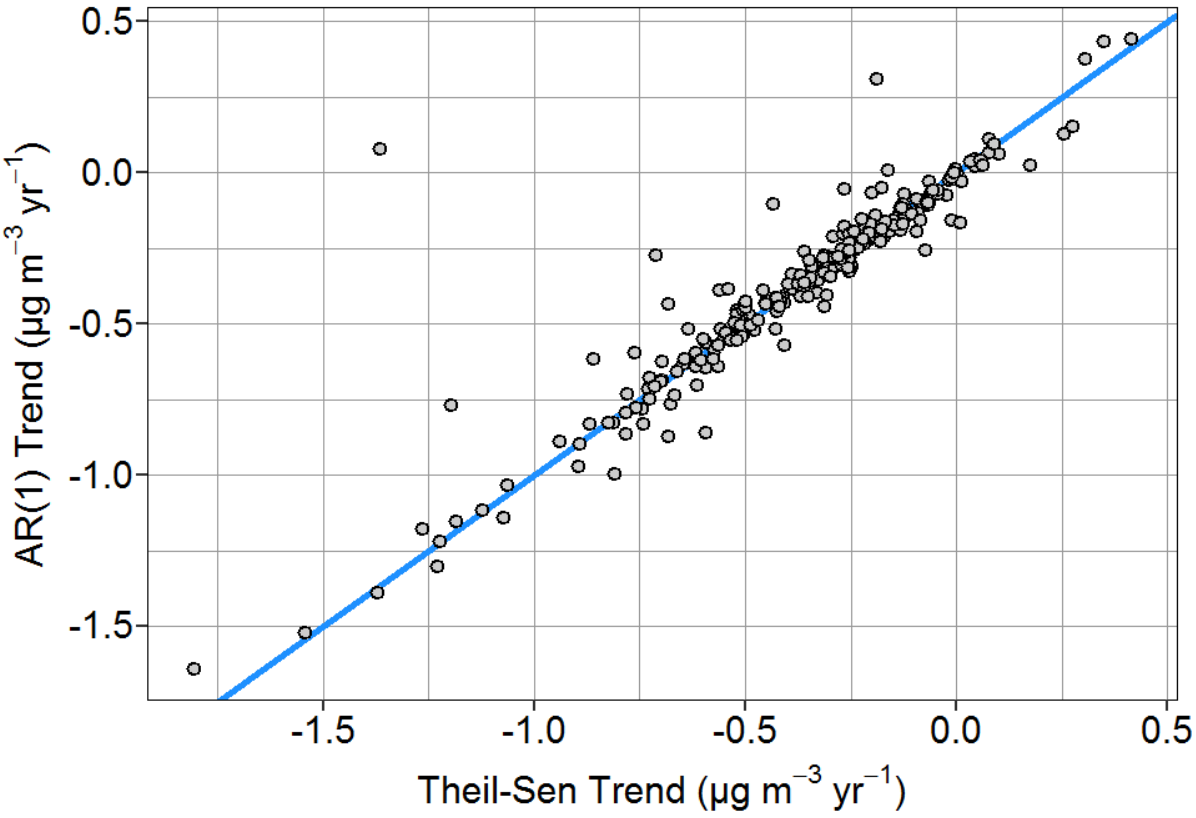

Figure S16: Comparison of the direction and magnitude of the trend in annual NO_2 concentrations between 2000 and 2014 at 259 sites across Europe using the Theil-Sen statistic and first order autoregressive (AR(1)) model.

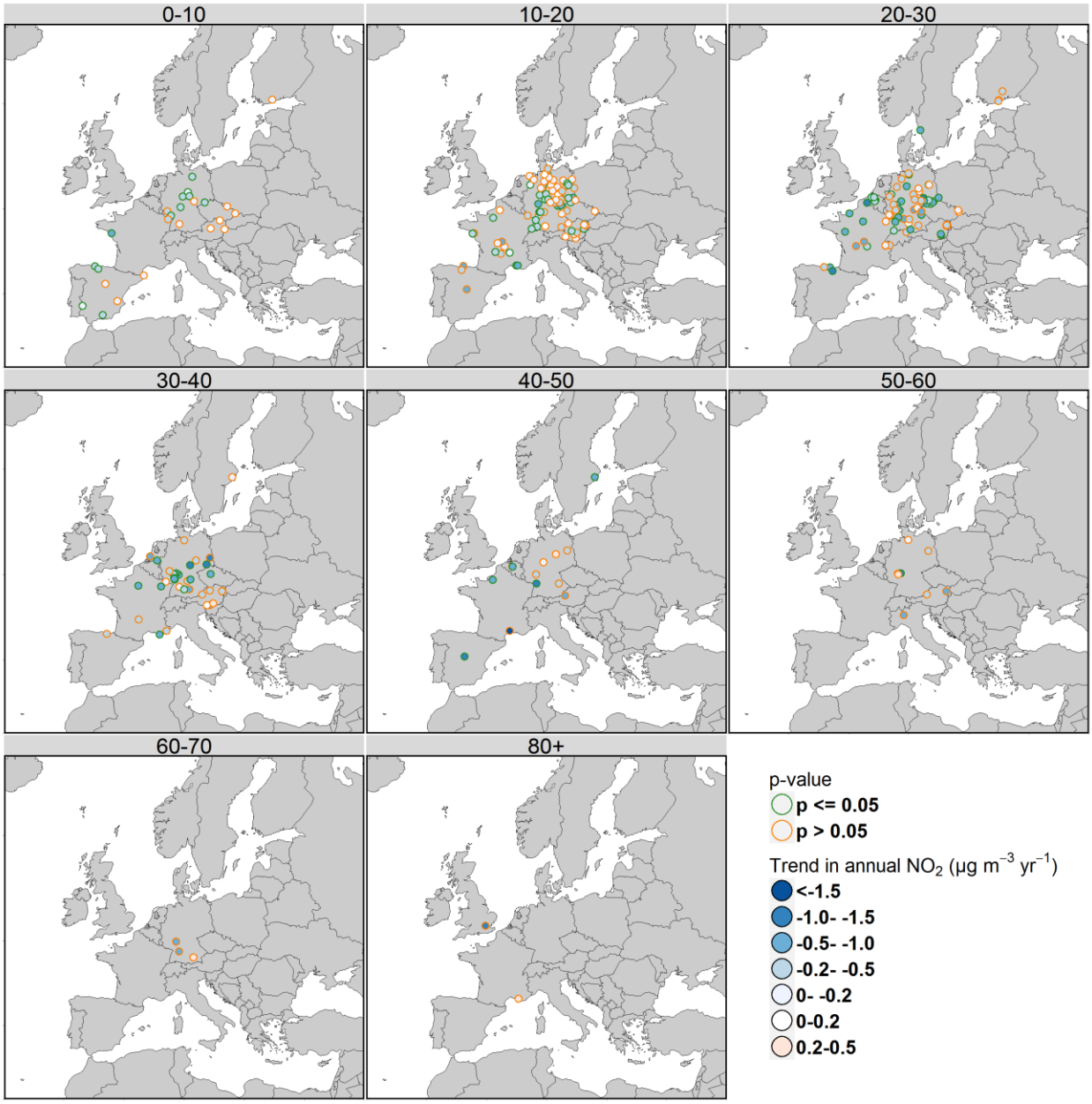

Figure S17: Magnitude and significance of trend in annual average NO_2 concentrations between 2000 and 2014, with sites separated into panels based on 2010-2014 average annual NO_2 concentrations (NO_{2AA}). The fill colour in each point denotes the magnitude and direction of the Theil-Sen trend at a site, and the outer colour denotes whether the trend was statistically significant ($p \leq 0.05$, green), or not statistically significant ($p > 0.05$, orange). Trend estimates were calculated using the Theil-Sen statistic and block bootstrapping.

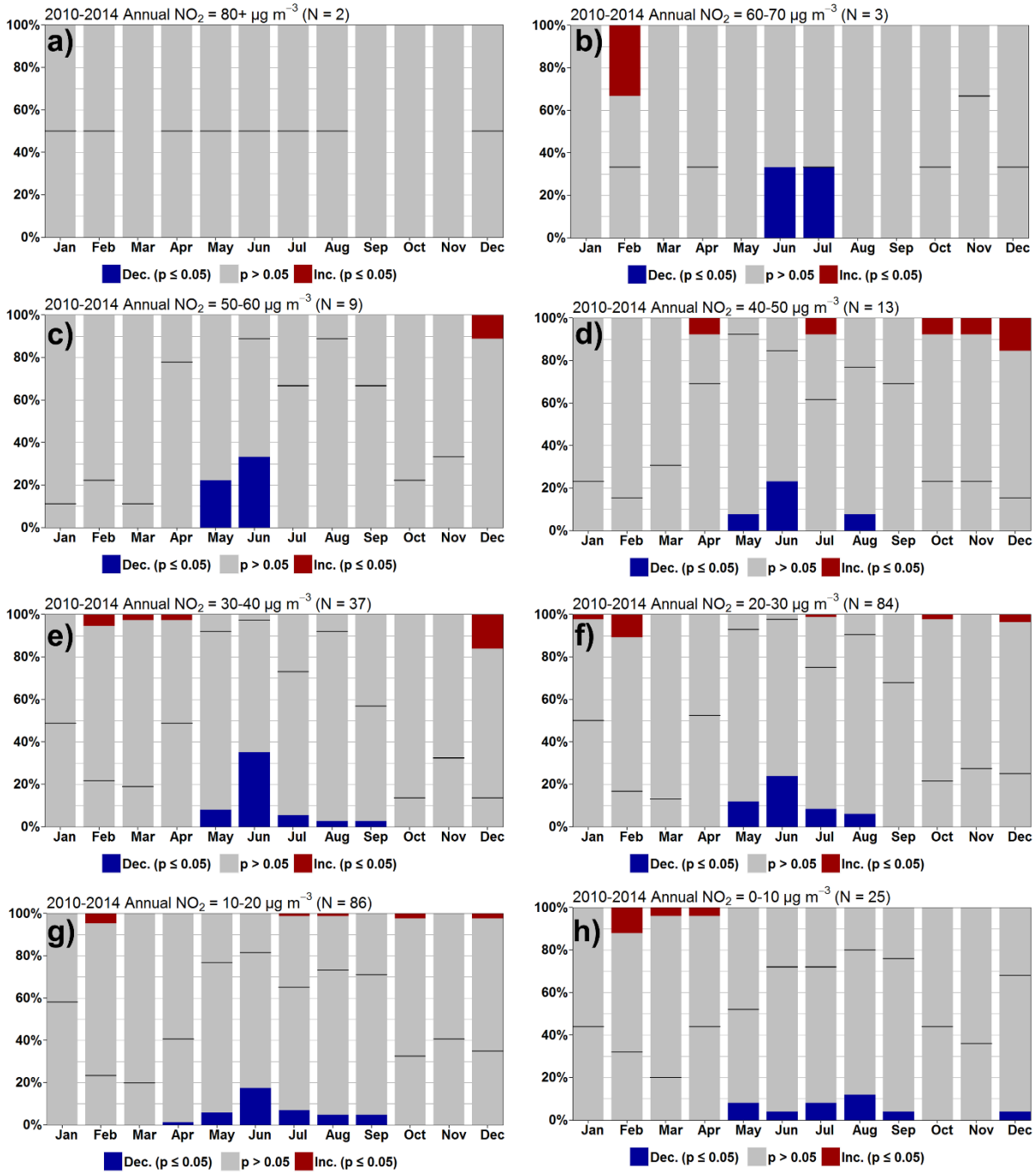

Figure S18: Proportion of sites with significant decreasing (blue), increasing (red) ($p \leq 0.05$), and non-significant (grey) trends in the monthly percentage contribution to annual average NO_2 between 2000 and 2014, for sites with 2010-2014 average annual NO_2 concentrations (NO_{2AA}) of a) >80 µg m^{-3}, b) 60-70 µg m^{-3}, c) 50-60 µg m^{-3}, d) 40-50 µg m^{-3}, 30-40 µg m^{-3}, 20-30 µg m^{-3}, 10-20 µg m^{-3}, 0-10 µg m^{-3}. Trend estimates were calculated using the Theil-Sen statistic and block bootstrapping. The black line represents the division between decreasing and increasing trends within the non-significant bar.

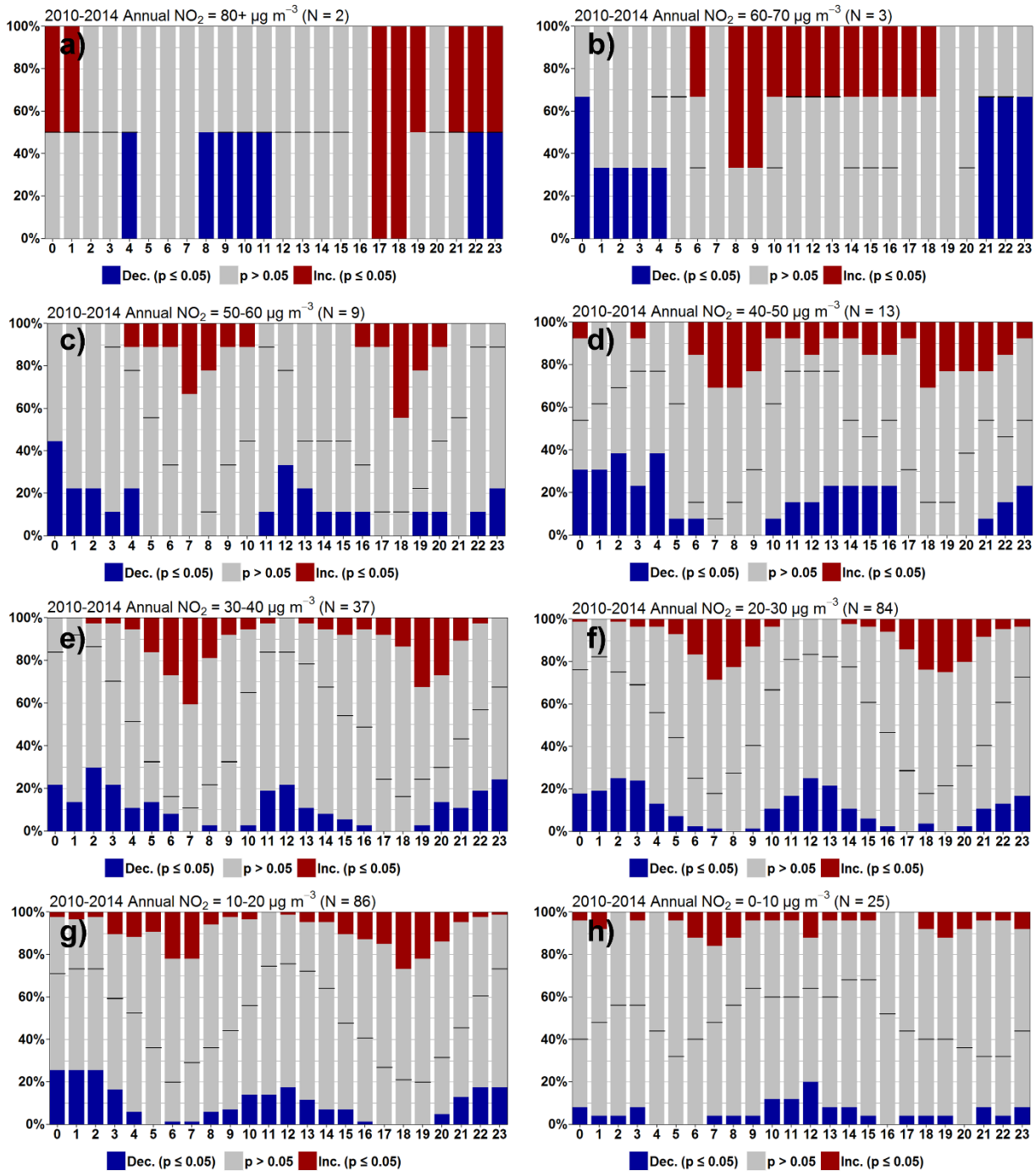

Figure S19: Proportion of sites with significant decreasing (blue), increasing (red) ($p \leq 0.05$), and non-significant (grey) trends in the percentage contribution of each hour of day to annual average NO_2 between 2000 and 2014, for sites with 2010-2014 average annual NO_2 concentrations (NO_{2AA}) of a) >80 µg m^{-3}, b) 60-70 µg m^{-3}, c) 50-60 µg m^{-3}, d) 40-50 µg m^{-3}, 30-40 µg m^{-3}, 20-30 µg m^{-3}, 10-20 µg m^{-3}, 0-10 µg m^{-3}. Trend estimates were calculated using the Theil-Sen statistic and block bootstrapping. The black line represents the division between decreasing and increasing trends within the non-significant bar.

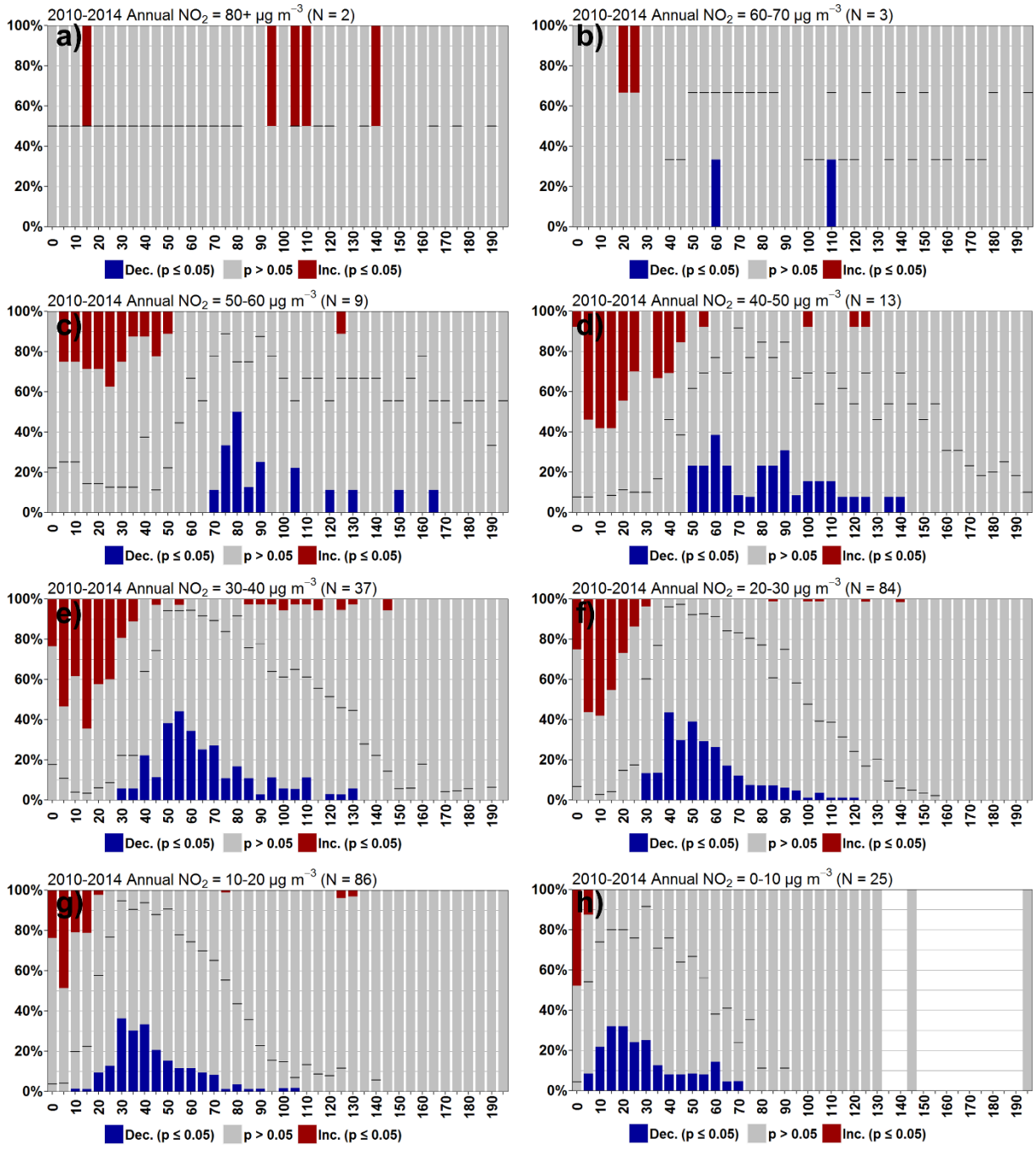

Figure S20: Proportion of sites with significant decreasing (blue), increasing (red) ($p < 0.05$), and non-significant (grey) trends in the percentage contribution from hourly NO_2 concentrations in 5 µg m^{-3} bins to annual average NO_2 between 2000 and 2014, for sites with 2010-2014 average annual NO_2 concentrations (NO_{2AA}) of a) >80 µg m^{-3}, b) 60-70 µg m^{-3}, c) 50-60 µg m^{-3}, d) 40-50 µg m^{-3}, 30-40 µg m^{-3}, 20-30 µg m^{-3}, 10-20 µg m^{-3}, 0-10 µg m^{-3}. Trend estimates were calculated using the Theil-Sen statistic and block bootstrapping. The black line represents the division between decreasing and increasing trends within the non-significant bar.